© 2015. Published by The Company of Biologists Ltd | Journal of Cell Science (2015) 128, 3489-3501 doi:10.1242/jcs.173922

RESEARCH ARTICLE

Regulation of the neuronal KCNQ2 channel by Src – a dual rearrangement of the cytosolic termini underlies bidirectional regulation of gating

Sivan Siloni*, Dafna Singer-Lahat*, Moad Esa, Vlad Tsemakhovich, Dodo Chikvashvili and Ilana Lotan‡

ABSTRACT

Neuronal M-type K^+ channels are heteromers of KCNQ2 and KCNQ3 subunits, and are found in cell bodies, dendrites and the axon initial segment, regulating the firing properties of neurons. By contrast, presynaptic KCNQ2 homomeric channels directly regulate neurotransmitter release. Previously, we have described a mechanism for gating downregulation of KCNQ2 homomeric channels by calmodulin and syntaxin1A. Here, we describe a new mechanism for regulation of KCNQ2 channel gating that is modulated by Src, a non-receptor tyrosine kinase. In this mechanism, two concurrent distinct structural rearrangements of the cytosolic termini induce two opposing effects: upregulation of the single-channel open probability, mediated by an N-terminal tyrosine, and reduction in functional channels, mediated by a C-terminal tyrosine. In contrast, Src-mediated regulation of KCNQ3 homomeric channels, shown previously to be achieved through the corresponding tyrosine residues, involves the N-terminal-tyrosine-mediated downregulation of the open probability, rather than an upregulation. We argue that the dual bidirectional regulation of KCNQ2 functionality by Src, mediated through two separate sites, means that KCNQ2 can be modified by cellular factors that might specifically interact with either one of the sites, with potential significance in the fine-tuning of neurotransmitters release at nerve terminals.

KEY WORDS: FRET, KCNQ2, Src, Gating, Open probability

INTRODUCTION

M-channels are members of the Kv7 family of voltage-dependent K^+ channels and are expressed predominantly in neuronal cells, with the most abundant subunits being KCNQ2 (Q2) and KCNQ3 (Q3) (Brown and Adams, 1980; Wang et al., 1998; Jentsch, 2000; Robbins, 2001; Klinger et al., 2011). Although heteromeric Q2–Q3 channels are expressed in the cell bodies and dendrites of many hippocampal and cortical neurons (Marrion, 1997; Cooper and Jan, 2003) and also in the initial segment of several neurons (Devaux et al., 2004; Chung et al., 2006; Klinger et al., 2011), where they control neuronal excitability by limiting repetitive firing (Hille, 1992; Dolly and Parcej, 1996; Miller, 2000; Millar et al., 2007; Regev et al., 2009), exclusive expression of Q2 subunits can be found in nerve terminals, where homomeric Q2 channels might directly regulate neurotransmitter release (Cooper and Jan, 2003; Devaux et al., 2004; Martire et al., 2004; Peretz et al., 2007). In humans, mutations in KCNQ2 are associated with benign (BFNC; Biervert et al., 1998; Singh et al., 1998) and non-benign (encephalopathy; Weckhuysen et al., 2012) neonatal forms of epilepsy.

M-channel gating is a target for extensive modulation. We previously put forward a mechanism for modulation of M-channel gating that was mediated by calmodulin (CaM) and syntaxin 1A (Syx, also known as STX1A) in *Xenopus* oocytes. This mechanism was solely targeted at Q2 subunits, downregulating the open probability of Q2 channels through a rearrangement in the relative orientation of their intracellular N- and C-termini (Etzioni et al., 2011). Such subunit specificity suggests selective targeting at presynaptic homomeric Q2 channels to directly regulate exocytosis, without interference with axonal Q2–Q3 heteromeric channels and neuronal firing properties (Regev et al., 2009). Another M-channels modulator is Src, a non-receptor tyrosine kinase, expressed by virtually all cells, including diverse neuronal cell types, where it is localized in dendrites, axons and nerve terminals (Sugrue et al., 1990). In rat sympathetic neurons, Src has been shown to suppress native M-currents (Gamper et al., 2003; Ebner-Bennatan et al., 2012) and, in CHO cells, Src associates with Q2, Q3, Q4 and Q5 subunits (Gamper et al., 2003) and downregulates the open probability of heteromeric Q2–Q3 channels (Li et al., 2004). However, the Gamper et al. study suggested that Src was only able to phosphorylate Q3, Q4 and Q5 subunits.

Intriguingly, two tyrosine residues located in opposite termini of the Q3 subunit have been shown to be involved in the Src action (Li et al., 2004), leading us to hypothesize that the modulation by Src might potentially involve crosstalk between the cytosolic termini, similar to the modulation by CaM and Syx. Furthermore, whereas in CHO cells Src has been reported to target Q3 and not Q2 (Gamper et al., 2003), a study in HEK cells has suggested that Src mediates a tonic increase in Q2 channel function (Jow and Wang, 2000). Taken together, we set out to study the Src action on Q2 in oocytes, hoping to find a new mode of Q2 gating regulation. Combining electrophysiological, fluorescence resonance energy transfer (FRET) and biochemical analyses, we characterize the effects of Src on homomeric Q2 wild-type (WT) and mutant channels and compare these results with those in respective Q3 homomeric channels.

The significance of this work is twofold. First, it puts forward a new mode of subunit-specific regulation of M-channels function that engages dual rearrangement of the relative orientation of the cytosolic termini, holding potential for Q2-specific fine-tuning of channel function. Second, although Src has been implicated in the regulation of presynaptic physiology, its role is not clear. This work suggests that Src-mediated regulation of Q2 homomers at presynaptic terminals might serve a role in the fine-tuning of transmitter release.

Department of Physiology and Pharmacology, Sackler School of Medicine, Tel-Aviv University, Ramat Aviv 69978, Israel.
*These authors equally contributed to this work

‡Author for correspondence (ilotan@post.tau.ac.il)

Received 6 May 2015; Accepted 26 July 2015

Journal of Cell Science (2015) 128, 3489-3501 doi:10.1242/jcs.173922

RESULTS

Recently, we have characterized the effects of CaM and Syx on Q2 and Q3 channels in *Xenopus* oocytes (Regev et al., 2009; Etzioni et al., 2011). We have described a mechanism for M-channel gating downregulation, specifically targeted at Q2, but not Q3, channel subunits, that involves rearrangement in the relative orientation of the intracellular N- and C-termini (Etzioni et al., 2011).

Here, we studied the regulation by Src of homomeric Q2 and Q3, WT and mutant, channels expressed in oocytes. Q3 carried an A315T point mutation, in the pore residue, to obtain better expression (Etxeberria et al., 2004). Given that we were interested in correlating electrophysiological measurements of channel function with FRET analysis of N-terminus–C-terminus interactions throughout this study, we only used double-fluorophore-labeled Q2 and Q3 subunits (with eCFP and eYFP genetically attached to the distal ends of their N-termini and C-termini; referred to hereafter as Q2 and Q3, respectively). The labeled channels have been previously shown to retain the WT voltage sensitivity, and responses to CaM and Syx (Etzioni et al., 2011), and were shown here to also retain the WT responses to Src (supplementary material Fig. S1).

Src reduces Q3 and, to a lesser extent, Q2 current amplitudes, and induces Q2 tyrosine phosphorylation

Previous functional studies in CHO cells have described that Src mediates a reduction in whole-cell currents of Q3 homomers but not Q2 homomers (Gamper et al., 2003), whereas another study in HEK cells has shown that Q2 currents are reduced upon treatment with Src inhibitors, suggesting that Src mediates a tonic increase of Q2 channel currents (Jow and Wang, 2000). Here, we addressed the effects of Src in oocytes by co-expressing Q2 or Q3 with a constitutively active Src kinase, Y527F Src (referred to hereafter as Src), which has been previously described to enhance Src-dependent effects (Gamper et al., 2003; Ebner-Bennatan et al., 2012). We detected a reduction of macroscopic current amplitudes not only of Q3 but also of Q2 (Fig. 1A,B). However, the extent of Q2 and Q3 current reduction was significantly different, whereas Src reduced Q3 currents by 57±6%, Q2 currents were only reduced by 38±4% (mean±s.e.m.; Fig. 1C). Src did not affect the voltage dependence of activation of either Q2 or Q3 channels (supplementary material Fig. S2). Importantly, the current reduction of both Q2 and Q3 channels were not accompanied by changes in peripheral channel expression, as determined by confocal imaging (Fig. 1D,E). Of note, such peripheral measurements have been previously shown to highly correlate with surface expression in oocytes (Regev et al., 2009; Rubinstein et al., 2009).

A previous co-immunoprecipitation analysis in CHO cells could detect a prominent association of Src with Q2 that was not less than that observed with Q3; however, Src-dependent tyrosine phosphorylation was only detected in Q3 (Li et al., 2004). However, in view of the reduction of Q2 currents mediated by Src in oocytes (Fig. 1A,B), we sought to detect Src-dependent tyrosine phosphorylation of Q2, similar to that determined for Q3. To this end, Q2 was immunoprecipitated with anti-Q2 antibody from lysates of oocytes expressing Q2, either alone or together with Src, and the precipitates were separated by SDS-PAGE and immunoblotted with either anti-phosphotyrosine antibody (to monitor phosphorylation level) or with anti-Q2 antibody (to monitor protein expression level). Notably, on top of Q2 basal tyrosine phosphorylation, as documented in CHO cells (Li et al., 2004), Src induced an increase in the Q2 phosphorylation signal without any concomitant increase in the level of protein expression (Fig. 1F). The increase in three independent experiments was small but highly significant ($P<0.01$). Taken together, the functional and the biochemical data indicate that Src reduces Q2 currents by phosphorylating channel tyrosine residues, similar to in Q3 (Li et al., 2004).

Src regulates the single-channel open probabilities of Q2 and Q3; however, it does so in opposite directions

The Src-mediated reduction of macroscopic currents without any concomitant change in peripheral channel expression (Fig. 1) suggests that single-channel characteristics, amplitude and/or open probability, are affected. Because it has been previously demonstrated that Src reduces the open probability (*Po*) of Q2–Q3 heteromeric channels in CHO cells (Li et al., 2004), we performed single-channel recordings in oocytes expressing either Q2 (Fig. 2A) or Q3 (Fig. 2B), with or without Src, at a saturating voltage of 0 mV, using the cell-attached configuration of the patch-clamp technique, as previously described (Etzioni et al., 2011). Surprisingly, the *Po* values of Q2 and Q3 homomers were oppositely affected by Src: Q2 *Po* increased (Fig. 2A) and Q3 *Po* decreased (Fig. 2B). Whereas the decrease in *Po* of Q3 by Src could be predicted from the reduced macroscopic currents by Src and was expected from the previous results obtained in CHO cells (Li et al., 2004), the increased *Po* of Q2 was unpredicted and puzzling, as it did not conform with the reduced Q2 macroscopic currents (Fig. 1A,B). Src did not affect the single-channel amplitudes (Fig. 2A,B, right-hand graphs).

Two tyrosine residues mediate the effect of Src on Q2

Being aware of the opposite effects of Src on Q2 and Q3 *Po* values, we first asked whether the tyrosine residues that mediate the effect of Src on Q2 correspond to those previously identified in Q3 (Li et al., 2004). Thus, we targeted the homologous tyrosine residues in Q2, Tyr-74 and Tyr-347, the first being localized to a conserved domain in the N-terminus, and the other localized to the first conserved domain in the C-terminus just after the S6 transmembrane domain (Q2 N-termini and Q2 C-termini tyrosine residues, correspondingly; Fig. 3A). Next, mirroring the previous investigation in Q3 (Li et al., 2004), we mutated the Q2 tyrosine residues, rendering them non-phosphorylatable, by Tyr-to-Phe mutation, generating Q2-Y74F and Q2-Y347F mutants. Both mutants expressed well and yielded macroscopic currents with a voltage sensitivity similar to that of WT channels (data not shown). Co-expression of the mutant channels with Src revealed that mutation of each one of the tyrosine residues was sufficient to abolish the Src-mediated reduction of current (Fig. 3B) without affecting peripheral channel expression (Fig. 3C), similar to what had been demonstrated for Q3 (Li et al., 2004). This requirement for both tyrosine residues to be phosphorylatable in order to support the Src-mediated effect on the Q2 macroscopic currents also held at the single-channel level, as the effect of Src on Q2 *Po* was blocked in either one of the mutants (Fig. 3D). These results indicate a similar mode of Src action on Q2 and Q3, requiring the phosphorylation of both of the widely separated N-terminal and C-terminal tyrosine residues that are homologous between the two channels. However, it did not provide a clue as to the opposite effects of Src on the *Po* values of the two channels, nor did it reconcile the opposite effect of Src on Q2 macroscopic currents and *Po* values.

Phosphomimetic substitutions at the N-terminal, but not at the C-terminal, tyrosine residues regulate Q2 and Q3 *Po* in opposite directions

To further explore the opposite effects of Src on Q2 and Q3 *Po*, we examined the consequences of a phosphomimetic mutation of Tyr-to-Asp substitution (imposing a negative charge that mimics

Journal of Cell Science (2015) 128, 3489-3501 doi:10.1242/jcs.173922

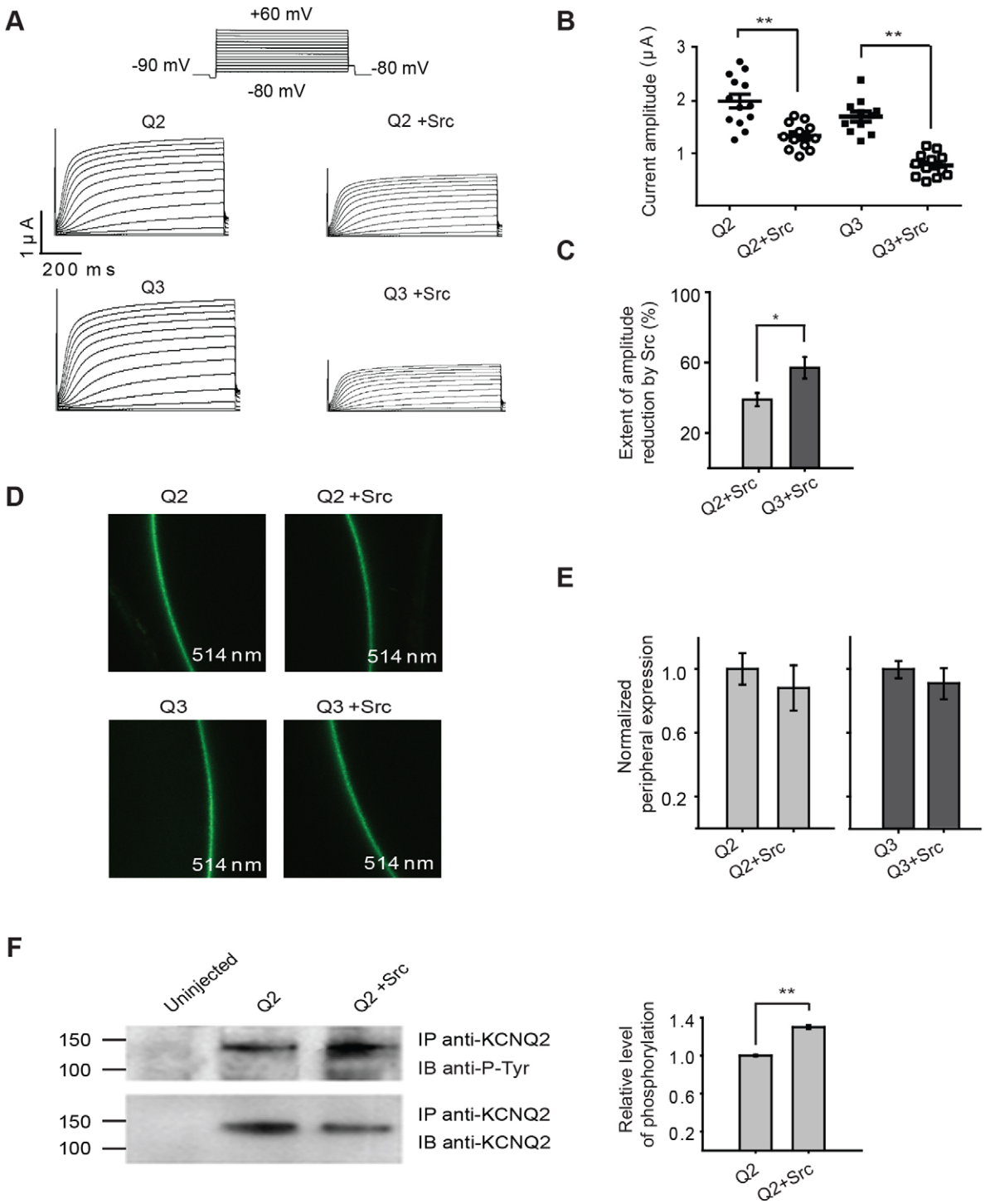

Fig. 1. Src reduces current amplitudes of Q2 and Q3 channels, without affecting peripheral channel expression. Reduction of Q2 currents is smaller than Q3 and involves tyrosine phosphorylation. (A,B) Src reduces current amplitudes of Q2 and Q3 channels. Representative current traces from single oocytes of the same batch (the inset in A shows the experimental protocol) and mean current amplitudes, evoked by a voltage step from a holding potential of –90 to 0 mV in one representative experiment (B; *n*=11–13), of Q2 and Q3 channels expressed in oocytes, alone or together with Src. (C) The current amplitude reduction by Src is smaller in Q2 then in Q3. Relative effect on current amplitude reduction, quantified as the fraction of current amplitude reduced in the presence of Src, derived from averaged current amplitudes of the channels, alone or coexpressed with Src, over five experiments (*n*=42–50 oocytes per group; *N*=5). (D,E) Src does not affect Q2 or Q3 peripheral expression. Confocal images taken under 514 nm laser excitations of a representative oocyte in a frame (D; the microscope settings were optimized to view the fluorescence of the oocytes of interest) and normalized mean peripheral protein levels were measured from confocal images of the same oocytes as in C (normalized to each channel expressed alone; E; *n*=42–50 oocytes per group; *N*=5) expressing Q2 or Q3 (which are fluorescently-labeled), alone or together with Src. (F) Q2 is constitutively tyrosine phosphorylated; phosphorylation is increased by Src. Left, Q2 proteins, alone or together with Src, were immunoprecipitated with anti-Q2 antibody (IP anti-Q2) and immunoblotted with anti-phosphotyrosine (IB anti-P-Tyr; upper panel), or with Q2 (IB anti-Q2; lower panel) antibodies. Molecular mass markers are denoted on the left. Right, histogram of the extent of phosphorylation normalized to the level of expression (quantified by ImageQuant) of Q2, derived from three independent experiments (*n*=27–36 oocytes per group; *N*=3). **P*<0.05; ***P*<0.01. Error bars indicate s.e.m. *n* denotes total number of oocytes per group; *N* denotes number of experiments in different batches of oocytes.

Journal of Cell Science (2015) 128, 3489-3501 doi:10.1242/jcs.173922

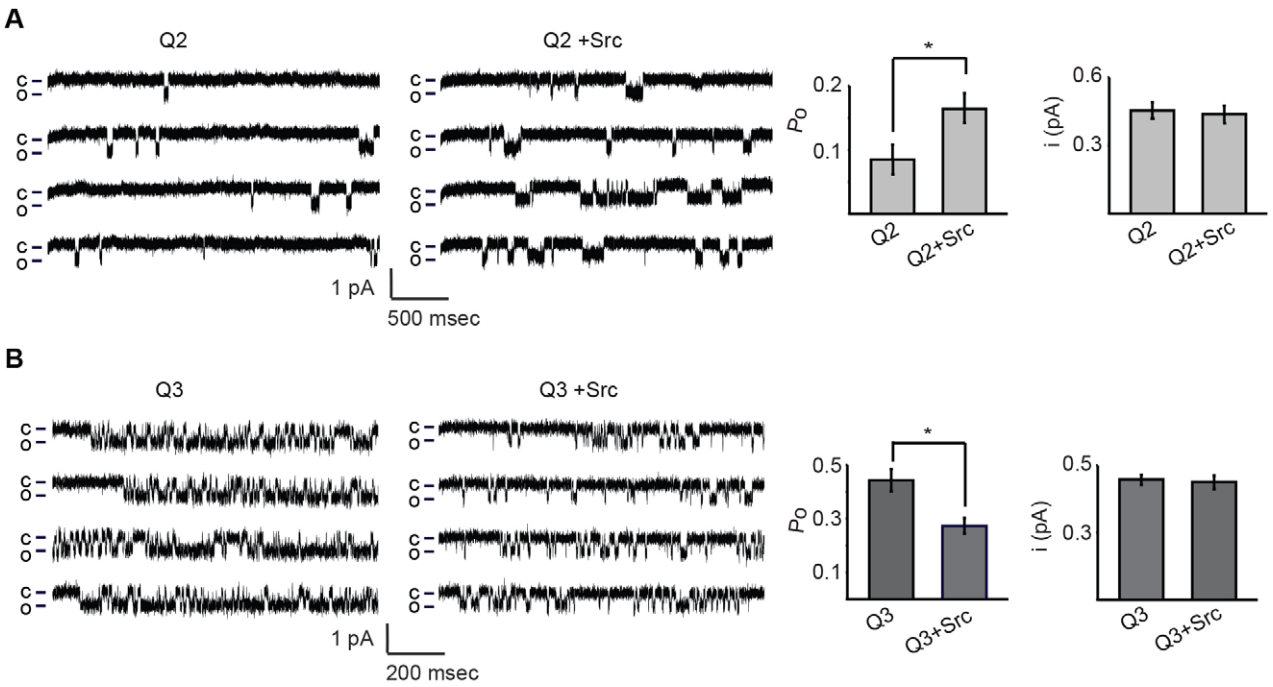

Fig. 2. Src increase single-channel *Po* of Q2 and decreases that of Q3. (A,B) Left, single-channel activity of Q2 (A) and Q3 (B) channels, with or without expressed Src, elicited by voltage steps from −90 to 0 mV. The presented oocyte patches contained a single Q2 or Q3 channel. Inward currents are shown as downward deflections. Right, mistograms of mean *Po* and mean amplitudes values of Q2 and Q3 with or without Src (n=4–5 patches per group, with up to three channels per patch). *P<0.05. Error bars indicate s.e.m.

that of a phosphate moiety) in each of the relevant tyrosine residues separately, both in Q2 and Q3. Strikingly, the C-terminal phosphomimetic mutants of both channels, Q2-Y347D and Q3-Y386D, did not yield any currents (Fig. 4A), although the peripheral cell expression of the proteins, as determined by confocal imaging, was substantial (Fig. 4B). We further substantiated the plasma membrane expression of the channels biochemically by SDS-PAGE analysis of channel proteins immunoprecipitated separately from manually dissected plasma membranes and cytosol (including internal membranes) (Ivanina et al., 1994) of oocytes expressing the corresponding proteins. This analysis confirmed that the expression of both Q2-Y347D and Q3-Y386D proteins was substantial in the plasma membranes (Fig. 4C). Although both biochemical and confocal analyses showed that the surface expression of Q3-Y386D was partially impaired compared with that of Q3 (Fig. 4B,C), this impairment could not account for the total loss of Q3-Y386D function. Taken together, we conclude that the phosphomimetic substitution at the C-terminal tyrosine residue renders both Q2 and Q3 surface channels inherently non-functional. In support, we could not detect any single-channel openings in membrane patches of these oocytes, attesting for Po=0 (data not shown). Interestingly, both the Q2-Y347D and Q3-Y386D mutated subunits exerted a dominant-negative effect on the heteromeric Q2–Q3 channel, yielding no whole-cell currents (supplementary material Fig. S3).

In contrast, the N-terminal phosphomimetic mutants of both channels yielded functional channels, however, with a marked difference between the two. Whereas Q2-Y74D yielded currents that were larger than those of WT Q2, Q3-Y104D yielded currents markedly smaller than those of WT Q3 (amplitudes were normalized to the peripheral protein expression; Fig. 4D). These results, together with the finding that the C-terminal phosphomimetic mutants are non-functional so that their *Po* is practically zero, suggested that the marked difference between the *Po* values of the channels (Fig. 2) might be conferred by their N-terminal tyrosine residues. Thus, we performed single-channel analysis of the N-terminal phosphomimetic mutants Q2-Y74D and Q3-Y104D. As expected, the N-terminal phosphomimetic mutations mimicked the effects of Src on the WT *Po* in both channels (see Fig. 2), increasing Q2 *Po* and decreasing Q3 *Po* (Fig. 4E), indicating that the differential effect of Src on *Po* values of the channels is indeed conferred by the N-terminal tyrosine residues.

The analyses of the phosphomimetic N-terminal and C-terminal mutations suggested that the effects of Src on WT Q2 and Q3 macroscopic currents (Fig. 1A–C) are the manifestation of the concurrent occurrence of two effects mediated by the phosphorylation of the C-terminal and N-terminal tyrosine residues. In Q2 the overlapping of two Src-mediated opposing effects, reduction of functional channels and increase of *Po*, gives rise to a small reduction of macroscopic currents. In Q3 the overlapping of two Src-mediated complementary effects, reduction of functional channels and decrease of *Po*, gives rise to a large reduction of macroscopic currents. This suggests that the larger reduction of WT Q3 macroscopic currents mediated by Src compared with that of WT Q2 (Fig. 1C) is the result of Src having opposite effects on the *Po* values of the two channels as mediated by the phosphorylation of their N-terminal tyrosine residues. To test this notion, we assayed the effect of Src on macroscopic currents of the N-terminal phosphomimetic mutants Q2-Y74D and Q3-Y104D, thus, circumventing the effects of Src mediated by phosphorylation of the N-terminal tyrosine residues, and solely assaying the effects mediated by phosphorylation of the C-terminal tyrosine residues. As expected, in this case, the Src-induced reductions of the mutant Q2 and Q3 channel currents (Q2-Y74D and Q3-Y104D) were of a similar extent (Fig. 4F; supplementary material Fig. S4).

Taken together, it emerges that Src primarily reduces both Q2 and Q3 currents through phosphorylation of their C-terminal tyrosine residues, whereas Src-induced phosphorylation of their N-terminal tyrosine residues regulates the current reduction in both channels, however, in opposite directions: increasing it in Q3 and decreasing it in Q2.

Journal of Cell Science (2015) 128, 3489-3501 doi:10.1242/jcs.173922

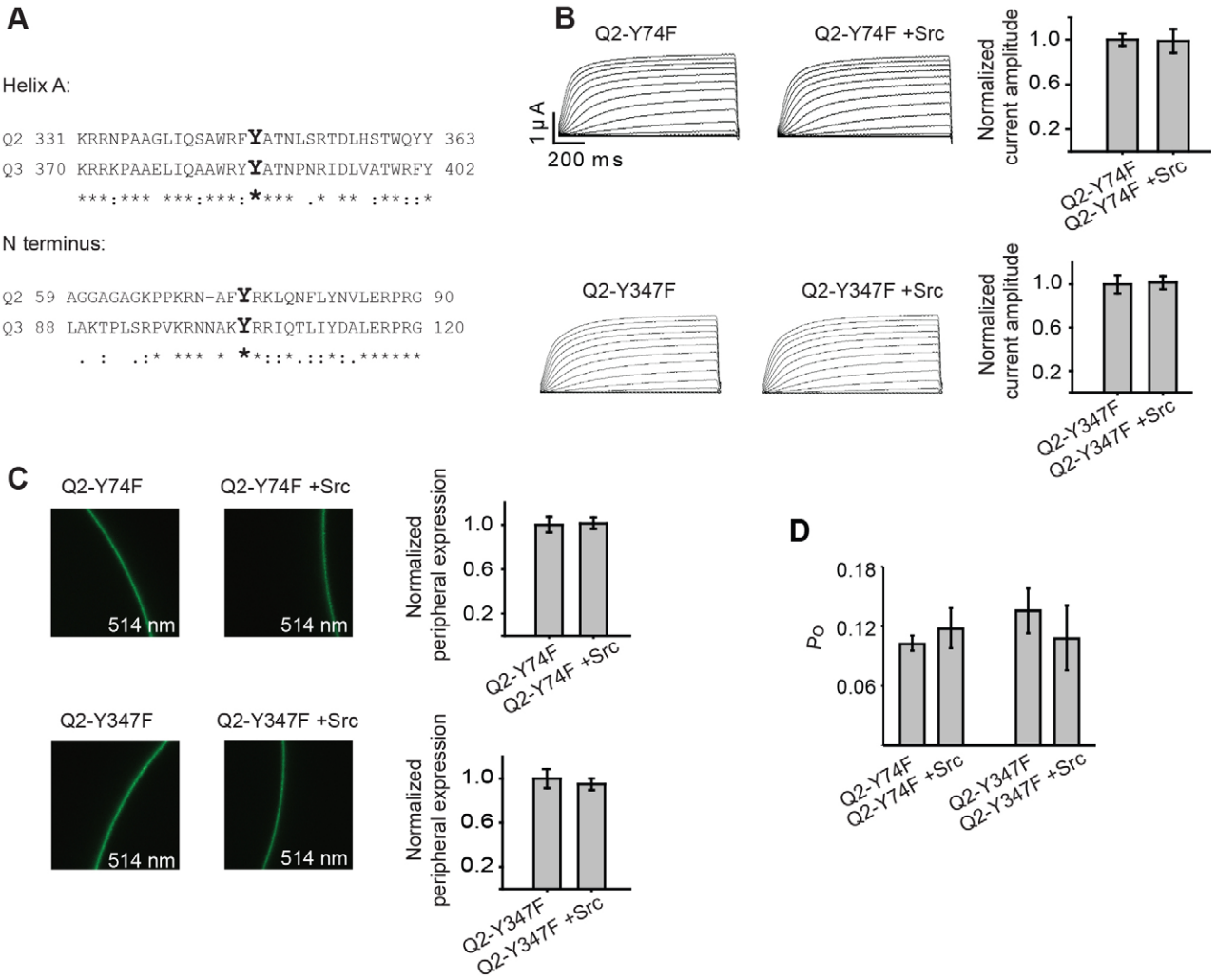

Fig. 3. Two tyrosine residues, at the N- and C-termini, mediate the effect of Src on Q2. (A) Alignment of part of the C-terminal helix A (upper panel) or the N-terminus (lower panel) of human Q2 and Q3, showing the tyrosine residues (Y) that are phosphorylated by Src. Alignment was performed using CLUSTAL W (1.83) multiple sequence alignment. *, identical or conserved residues; ':', conserved substitutions; '.', semi-conserved substitutions. (B) Src does not affect current amplitudes of mutated Q2 channels in which tyrosine residues Y74 or Y347 were mutated to a phenylalanine residue (Q2-Y74F or Q2-Y347F, respectively). Left, representative current traces of Q2-Y74F (upper panel) and Q2-Y347F (lower panel), alone or coexpressed with Src, in oocytes of the same batch. Right, normalized averaged current amplitudes, evoked by a voltage step from a holding potential of –90 to 0 mV, of the channels, alone or coexpressed with Src (normalized to each channel expressed alone; n=38–26; N=3). (C) Src does not affect Q2-Y74F or Q2-Y347F peripheral expression. Left, confocal images taken under 514-nm laser excitations of a representative oocyte in a frame. The microscope settings were optimized to view the fluorescence of the oocytes of interest. Right, normalized mean peripheral protein levels measured from confocal images of the same oocytes as shown in B (normalized to each channel expressed alone; right panels; n=38–26; N=3), expressing Q2-Y74F or Q2-Y347F (which are fluorescently labeled), alone or together with Src. (D) Src does not affect the *Po* of Q2-Y74F and Q2-Y347F. *Po* values Q2-Y74F or Q2-Y347F with or without Src. Error bars indicate s.e.m. n denotes total number of oocytes per group; N denotes number of experiments in different batches of oocytes.

Po regulation by Src requires both the N-terminal and C-terminal tyrosine residues and N-terminus–C-terminus compatibility

The ability of Src to increase Q2 *Po* (Fig. 2) requires that the C-terminal tyrosine residue be present so it can be phosphorylated (Fig. 3D; Q2-Y347F), although this can be mimicked by the phosphomimetic substitution of the N-terminal tyrosine alone (Fig. 4E; Q2-Y74D). We tested whether this requirement reflects constraints of the intrinsic channel gating machinery by analyzing the *Po* of the double mutant Q2-Y74D; Q2-Y347F. In spite of the non-phosphorylatable substitution at the C-terminus of this mutant, its *Po* was significantly higher than that of WT Q2 (Fig. 5A), owing to the N-terminal phosphomimetic substitution, as was observed with the single Q2-Y74D mutant (Fig. 4E). We conclude that the requirement for two intact tyrosine residues at the N-termini and C-termini is set by Src itself and not the gating machinery, vouching for a specific N-terminus–C-terminus platform that is required for the functional interaction of Src with the channels. We set out to further explore this using chimeric Q2–Q3 subunits with exchanged N-terminal and C-terminal sequences. First, we tested the effect of Src on $Q2_{(helixA)}$, a Q2 subunit in which helix A, the membrane-proximal C-terminal helix that contains the C-terminal tyrosine, was exchanged with the corresponding helix A of Q3 (Etzioni et al., 2011). As expected in light of the very high similarity between the two helices (Fig. 3A), the Src-induced increase of Q2 *Po* was maintained (Fig. 5B). Broadening the exchanged sequences, we next tested two other chimeras denoted $Q2_{(223)}$ and $Q2_{(322)}$, Q2 subunits in which the whole C-terminus or whole N-terminus [$Q2_{(223)}$ is composed of Q2 (amino acids 1–310) and Q3 (amino acids

Journal of Cell Science (2015) 128, 3489-3501 doi:10.1242/jcs.173922

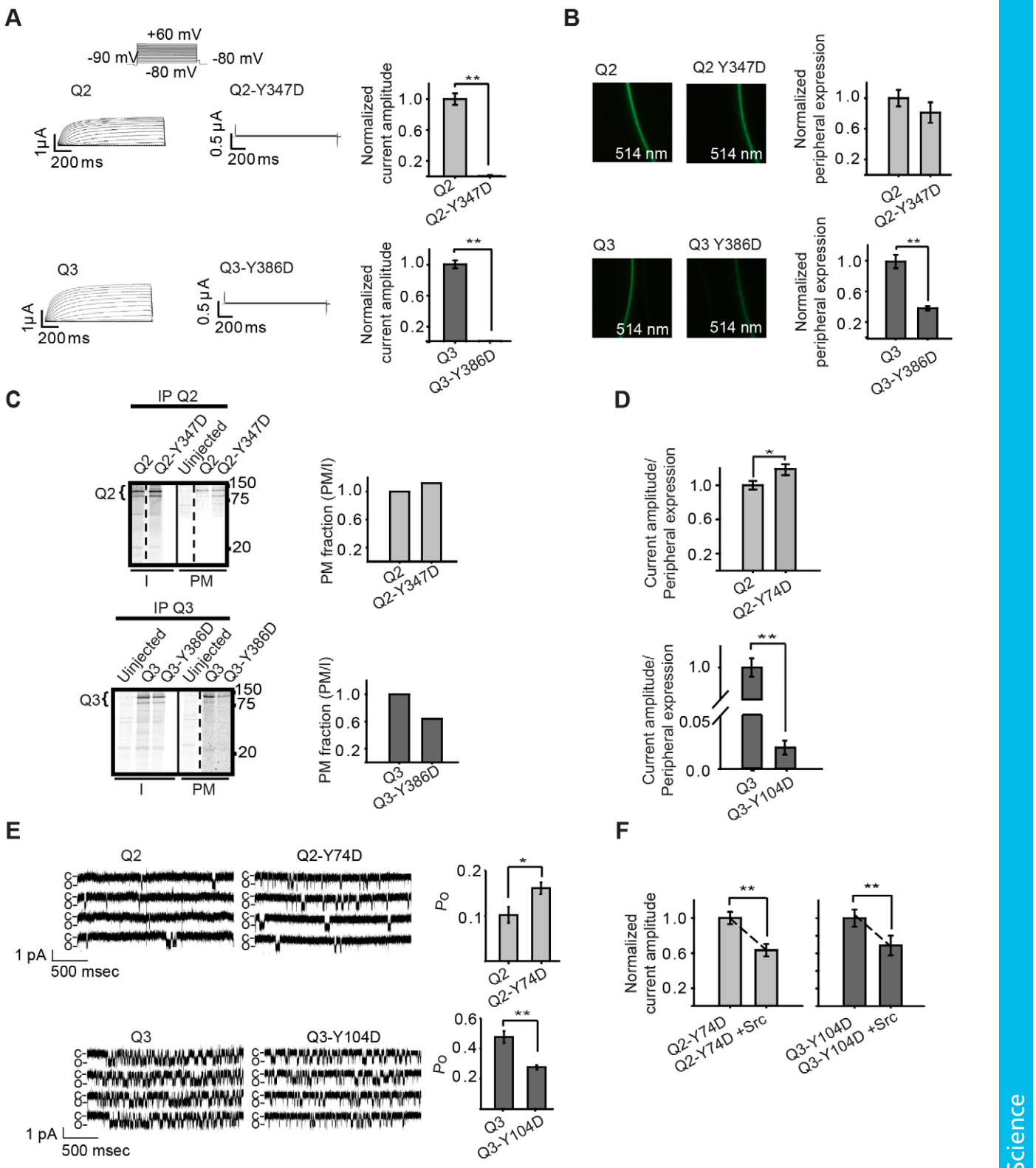

Fig. 4. See next page for legend.

347–872), and $Q2_{(322)}$ is composed of Q3 (amino acids 1–120) and Q2 (amino acids 89–845)], respectively, were replaced with those of Q3. Strikingly, in both cases, the Src-induced increase in the Q2 *Po* was totally eliminated (Fig. 5C). Taken together, these results suggest that compatible Q2 N-termini and C-termini form a defined cytosolic structural platform for Src.

Regulation of N-terminus–C-terminus interactions accompany and positively correlate with regulations of *Po*; the regulations are in different directions in Q2 compared with Q3

The above results suggest the involvement of a crosstalk between closely positioned N- and C-termini (N-terminus–C-terminus interaction) for the effect of Src on *Po*. Indeed, channel gating

Journal of Cell Science

Journal of Cell Science (2015) 128, 3489-3501 doi:10.1242/jcs.173922

Fig. 4. Phosphomimetic substitutions of N-terminal tyrosine residues mediate differential effects on Q2 and Q3 channels, whereas phosphomimetic substitutions of C-terminal tyrosine residues render plasma-membrane Q2 and Q3 channels non-functional.
(A) Phosphomimetic substitution of the C-terminal tyrosine residues of Q2 and Q3 render plasma membrane non-functional channels. Left, representative current traces from single oocytes (the inset shows the experimental protocol). Right, normalized mean current amplitudes evoked at 0 mV (n=15–17; N=2) of Q2, Q2-Y347D, Q3 and Q3-Y386D channels expressed in the same batches of oocytes. (B) Effects of phosphomimetic substitutions of the C-terminal tyrosine residues on peripheral expression of the channels. Left, confocal images taken under 514-nm laser excitation of a representative oocyte in a frame. The microscope settings were optimized to view the fluorescence of the oocytes of interest. Right: normalized mean peripheral protein levels measured from confocal images of the same oocytes as shown in A (normalized to WT Q2 or Q3 channels, respectively; n=15–17; N=2), expressing Q2, Q2-Y347D, Q3 and Q3-Y386D (which are fluorescently labeled). (C) Effects of phosphomimetic substitutions of the C-terminal tyrosine residues on plasma membrane expression of the channels. Left, digitized PhosphorImager scan of SDS-PAGE analysis of [^{35}S]Met/Cys-labeled Q2, Q2-Y347D, Q3 or Q3-Y386D proteins, immunoprecipitated by Q2 or Q3 antibodies, respectively, from manually-dissected 40 plasma membranes (PM) or three cytosols including internal membranes (I). Dashed lines denote non-adjacent lanes. Migration of standard molecular mass markers is denoted on the right. Right, histograms of ratios of band densities of the channel proteins expressed in PM versus I (PM fraction; quantified by ImageQuant). (D) Phosphomimetic substitutions of the N-terminal tyrosine residues of Q2 and Q3 reduces Q3, but increases Q2, current amplitudes. Ratios between current amplitudes evoked at 0 mV and peripheral expressions, measured from confocal images (as in B), of the same oocytes expressing Q2, Q2-Y74D, Q3 or Q3-Y386D (n=27–32; N=3).
(E) Phosphomimetic substitutions of Q2 N-terminal tyrosine residues increases the Q2, but decreases the Q3, Po. Left, single-channel activity of Q2, Q2-Y74D, Q3 and Q3-Y104D elicited by voltage steps from –90 to 0 mV. The presented oocyte patches contained a single channel. Right, histograms of mean Po values (n=4–7 patches per group, with up to three channels per patch). (F) Src decreases current amplitudes of the N-terminal tyrosine residues phosphomimetic Q2 and Q3 mutants. Shown are normalized mean current amplitudes, evoked at 0 mV, in oocytes of the same batches (n=18–19; N=2) of Q2-Y74D and Q3-Y104D, alone or coexpressed with Src. Note the dashed slope lines representing a similar effect of Src (n=18–19; N=2). *P≤0.05; **P≤0.01. Error bars indicate s.e.m. n denotes total number of oocytes per group; N denotes number of experiments in different batches of oocytes.

modulators have been shown to alter N-terminus–C-terminus interactions (Lippiat et al., 2002; Tsuboi et al., 2004; Lvov et al., 2009; Etzioni et al., 2011). Specifically, constitutive N-terminus–C-terminus interactions have been characterized in Q2 and Q3, and have been shown in Q2 to be modulated by CaM and syntaxin, accompanying changes in Q2 Po (Etzioni et al., 2011). Thus, we set out to explore whether the Src-induced gating regulation is accompanied by specific changes in the N-terminus–C-terminus interaction within Q2 and Q3 (Fig. 6). We used FRET analysis to monitor the N-terminus–C-terminus proximity in functional channels under physiological conditions. Crosstalk was assessed by the apparent FRET efficiency between eCFP and eYFP (as performed previously; Lvov et al., 2009; Etzioni et al., 2011), which are genetically attached to the distal ends of N-terminus and C-terminus, respectively, of Q2 and Q3. As was established previously (Etzioni et al., 2011), oocytes expressing Q2 or Q3 channels exhibited FRET (Fig. 6A–C), vouching for constitutive N-terminus–C-terminus interactions in both channels. It should be noted that, although being small, the FRET signals of the two channels are substantial and persistent, and have been previously shown to be similar to that of a positive control (a strong FRET) and significantly different from a negative control (of no FRET) (Etzioni et al., 2011). Furthermore, FRET analysis of the effect of Src revealed isoform-specific regulations of the N-terminus–C-terminus interactions within Q2 and Q3, similar to the Src-induced gating regulation. Namely, co-expressed Src significantly increased the FRET in Q2 but significantly decreased the FRET in Q3 (Fig. 6A–C). We further asked whether the requirement of the two tyrosine residues for the Src-mediated effect on the macroscopic currents and Po values also holds for the Src-mediated effect on the N-terminus–C-terminus interactions. Indeed, FRET analysis showed that Src had no significant effect on either of the non-phosphorylatable mutants (Q2-Y74F and Q2-Y347F; Fig. 6D,E), attesting for the requirement for both tyrosine residues for the effect of Src on the channel.

Next, we tested the effect of phosphomimetic substitutions at the N-terminal and C-terminal tyrosine residues on the N-terminus–C-terminus interaction of Q2 and Q3. FRET analysis of Q2-Y74D and Q3-Y104D revealed isoform-specific effects of the phosphomimetic substitutions, with increased FRET in Q2 and decreased FRET in Q3 (Fig. 6F,G), similar to the Src-mediated effects on the corresponding WT channels (Fig. 6A–C). Strikingly, FRET analysis (Fig. 6H,I) of the non-functional Q2-Y347D and Q3-Y386D channels (see Fig. 4A–C) revealed no FRET in both channels. Namely, loss of the constitutive N-terminus–C-terminus interaction, mediated by the C-terminal tyrosine residue, underlies loss of function of both Q2 and Q3 channels.

Notably, the effects on FRET induced by Src or by the phosphomimetic substitution of the N-terminal tyrosine residues clearly correlated with those on Po. Namely, enhanced FRET paralleled enhanced Po, and vice versa, decreased FRET paralleled decreased Po (compare Fig. 6 with Fig. 2 and Fig. 4E). In addition, the zero change in FRET paralleled a zero change in Po (compare Fig. 6D,E with Fig. 3D). Taken together, the Po and FRET analyses reveal a mode of channel gating regulation in which regulation of the N-terminus–C-terminus interaction positively correlates with the single-channel gating regulation. Notably, this correlation is different from the described regulations by CaM and Syx of Q2 because there is an inverse correlation between changes in N-terminus–C-terminus interaction and gating, with an increase in FRET was accompanied by a reduction in Po (Etzioni et al., 2011).

The effect of Src on Q2 is mediated by concurrent phosphorylation of both tyrosine residues

All aspects of the Src-mediated effects, regarding macroscopic current, single-channel gating and N-terminus–C-terminus interaction, seem to require the presence of both the N-terminal and C-terminal tyrosine residues. Thus, an important mechanistic question arises as to whether the Src action is mediated through the concurrent phosphorylation of both tyrosine residues. We addressed this question with regard to Q2 by integrating the two experimental approaches implemented in our study, using FRET and Po analyses, according to the following considerations: (1) comparison of the N-terminal tyrosine phosphomimetic mutant with WT channels, providing a ratio between fold increases in FRET and the Po of the mutant channels, which should serve as a good estimate of the effect of phosphorylation by Src of the N-terminal tyrosine residue; and (2) that the C-terminal tyrosine phosphomimetic substitution generates non-functional channels with zero Po and zero FRET. This suggests that phosphorylation by Src of the C-terminal tyrosine residue is reflected only in a reduction in FRET with no effect on Po given that FRET analysis corresponds to all peripheral channels, functional and non-functional, whereas Po analysis only corresponds to functional channels. Taken together, it is predicted that concurrent phosphorylation of both tyrosine residues by Src will result in a ratio between the fold-increases in FRET and Po that is significantly smaller than that determined for the Q2 N-terminal phosphomimetic substitution. As shown in Fig. 7, we tested this

Journal of Cell Science (2015) 128, 3489-3501 doi:10.1242/jcs.173922

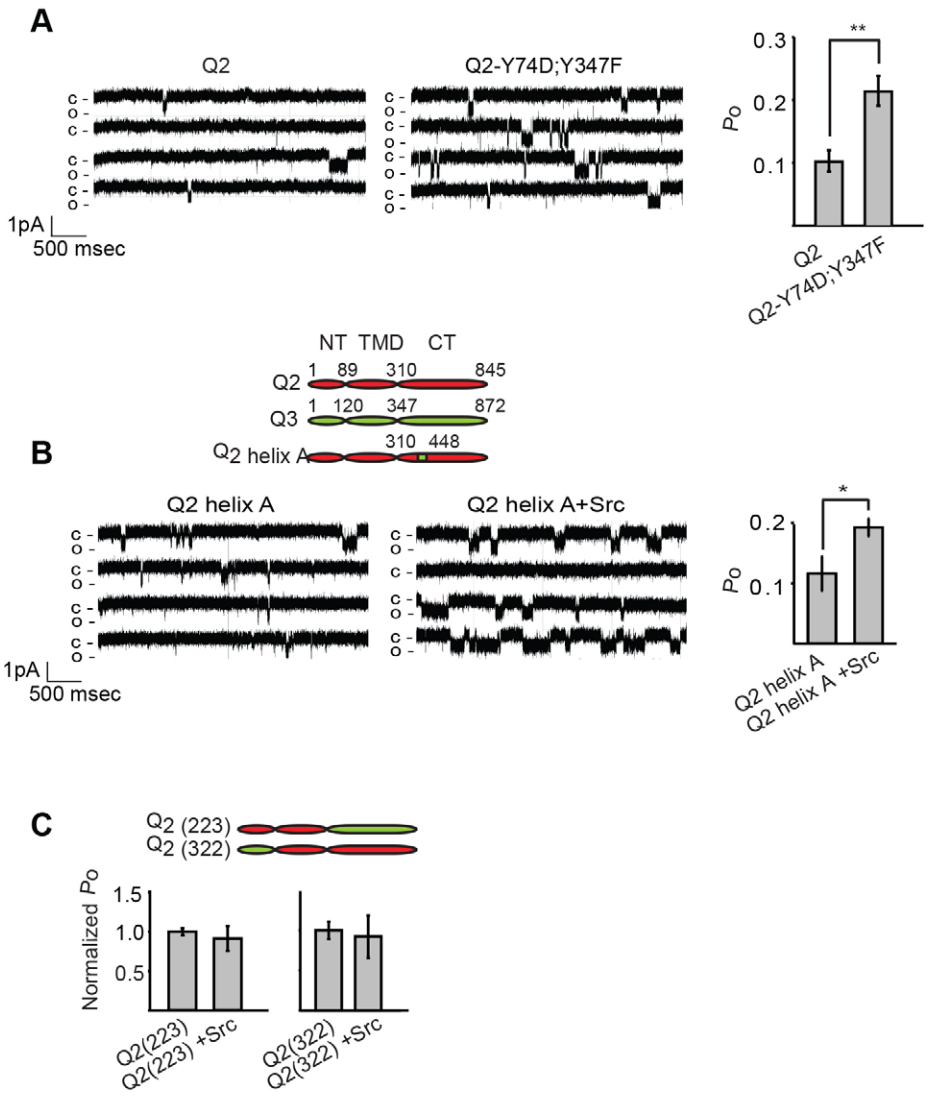

Fig. 5. Src regulation of Q2 *Po* requires the availability of both N-terminal and C-terminal tyrosine residues and their compatibility. (A) Src increases *Po* values of a double mutant with phosphomimetic substitutions of the N-terminal and C-terminal tyrosine residues (Q2-Y74D;Y347F; n=8–15 patches per group). (B) Src increases the *Po* of a chimeric Q2 channel in which helix A of Q2, which contains the C-terminal tyrosine, was exchanged for the corresponding helix A of Q3 (Q2 helix A; n=6–8 patches per group). Inset, schematic representations of Q2, Q3, and Q2 helix A. (C) Src does not affects *Po* of chimeric Q2 channels in which whole C-terminal (left panel) or N-terminal (right panel) ($Q2_{(223)}$ or $Q2_{(322)}$, respectively) were replaced with that of Q3. (n=8–13 patches per group) Inset, schematic representations of $Q2_{(223)}$ or $Q2_{(322)}$. *$P\leq0.05$; **$P<0.01$. Error bars indicate s.e.m.

prediction by analyzing changes in *Po* and FRET induced by the N-terminal phosphomimetic substitution and by Src in oocytes of the same batch, using a two-way ANOVA analysis, as detailed in the Fig. 7 legend. In accordance with our prediction, whereas the fold increases in Q2-Y74D *Po* and FRET values over those of WT channels were similar (1.52±0.40 and 1.54±0.33, respectively; mean±s.e.m., $P>0.05$; shown in Fig. 7 as white symbols), the fold increases of *Po* and FRET values induced by Src action on Q2 WT were not similar (Fig. 7; black symbols) – the fold-increase in FRET (1.37±0.31) was smaller than that in *Po* (1.96±0.52). Taken together, we conclude that the effect of Src on Q2 reflects the overlapping of two concurrent effects that are mediated by the phosphorylation of the N-terminal tyrosine residue to increase *Po*, and by the phosphorylation of the C-terminal tyrosine residue to generate non-functional channels.

DISCUSSION

In this study, we characterize a new intricate mechanism utilized by Src to regulate Q2 channel function. Src targets two separate tyrosine residues, one at the N-terminus and one at the C-terminus, each of which mediates distinct rearrangements within the channel cytosolic structure that give rise to respective upregulation of single-channel gating (*Po*) and downregulation of the availability of functional channels, with both effects occurring concurrently. The dual action of Src through the two tyrosine residues confers bidirectional regulation of Q2 channel function (see below). The bidirectional Q2 gating regulation mediated by Src has potential physiological significance in the fine-tuning of neurotransmitters release at nerve terminals (see below).

Furthermore, comparison with the Src-mediated regulation of Q3 homomeric channels revealed that there was isoform-specific regulation. In Q3, the respective N-terminal tyrosine mediated cytosolic rearrangements opposite to those mediated by the Q2 N-terminal tyrosine, giving rise to downregulation of single channel gating, in contrast to the upregulation in Q2, whereas the respective Q3 C-terminal tyrosine mediated downregulation of the availability of functional channels, similar to Q2. The dual action of Src through the two tyrosine residues confers robust downregulation of Q3 channel function. Namely, isoform specificity is conferred by the differential effects of Src on Q2 and Q3, in contrast to CaM and Syx, which gain isoform specificity by restricting their effects only to Q2 (Etzioni et al., 2011).

Intricate regulation of M-channels gating by Src: bi-functionality and isoform-specific regulation of gating

The results suggest that there is a two-faceted mechanism for the Src-mediated M-channel regulation. The first facet is bi-functionality, in the sense that Src action entails concurrent

Journal of Cell Science (2015) 128, 3489-3501 doi:10.1242/jcs.173922

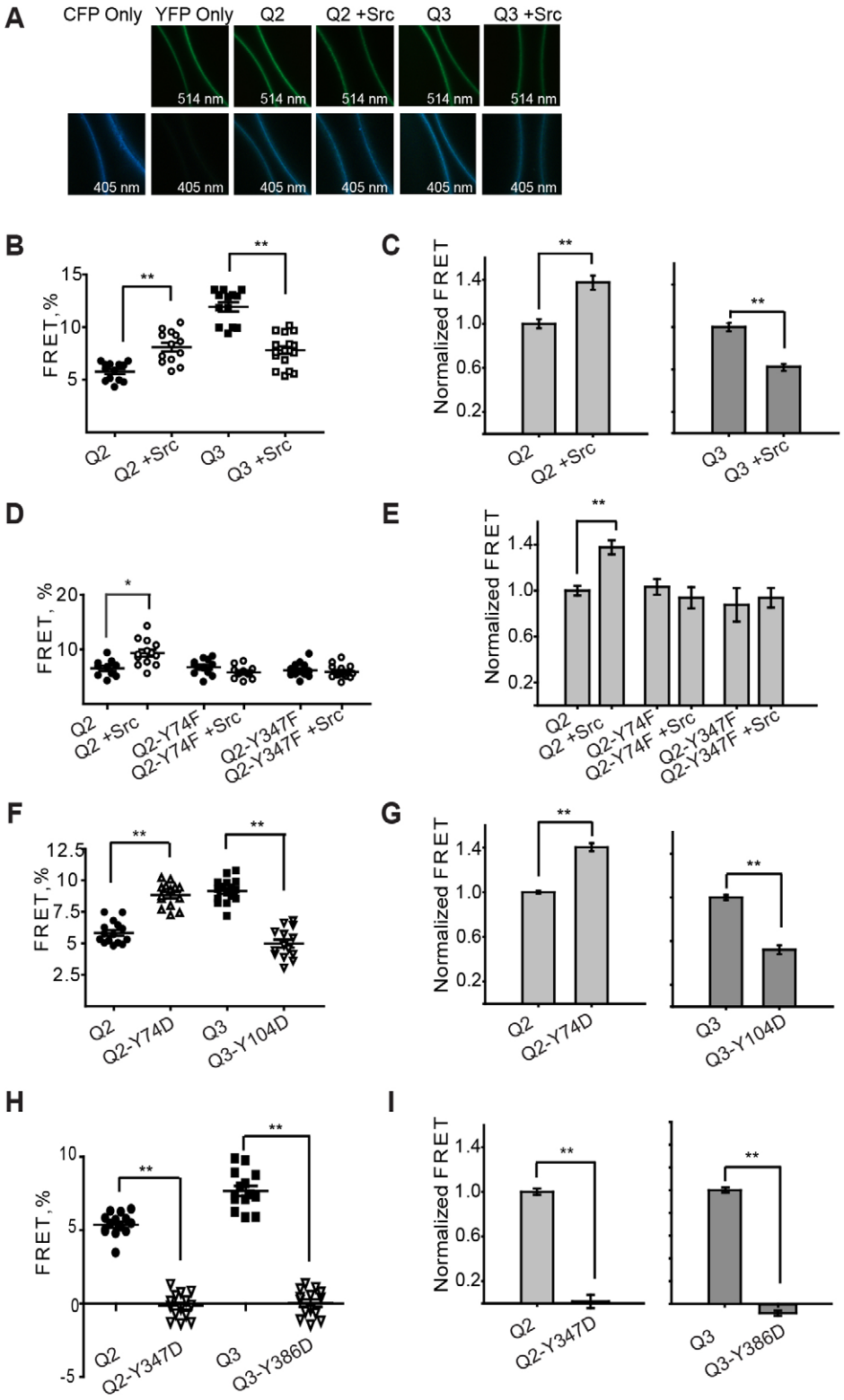

Fig. 6. Src and tyrosine mutations differently affects the N-terminus–C-terminus interaction of Q2 and Q3. (A) Confocal images of two representative oocytes in a frame expressing Q2 and Q3 channels, labeled with eCFP at the distal end of the N-terminal and with eYFP at the distal end of the C-terminal, expressed alone or together with Src, excited with a 405-nm or with 514-nm laser. (B) Src increases FRET between the Q2 N-terminus and C-terminus, but reduces FRET between the Q3 N-terminus and C-terminus. A representative experiment showing FRET between the N-terminal and C-terminal of Q2 or Q3, alone or coexpressed with Src (n=13–15). (C) Mean FRET (normalized to that of Q2, left panel, or Q3, right panel, derived from three experiments; n=23–37). (D) Src does not affect FRET between the N-terminus and C-terminus of Q2 Tyr-to-Phe mutated channels. A representative experiment showing FRET between Q2-Y74F and Q2-Y347F alone or coexpressed with Src (n=10–13). (E) Mean FRET (normalized to that of Q2) derived from two experiments as in D (n=23–26). (F) Tyr-to-Asp mutation at the N-terminus increases FRET between the N-terminus and C-terminus of Q2, but reduces FRET between the N-terminal and C-terminal of Q3. A representative experiment showing FRET between N-terminus and C-terminus of Q2-Y74D or Q3-Y104D (n=15–16). (G) Mean FRET normalized to that of Q2 (left panel) or Q3 (right panel) derived from three experiments as in F (n=41-47). (H) No FRET is apparent between the Q2 N-terminus and C-terminus upon the of Tyr-to-Asp mutation at the C-terminal of Q2 or Q3. A representative experiment showing FRET signals between the N-terminus and C-terminus of Q2-Y347D or Q3-Y386D (n=14). (I) Mean FRET (normalized to that of Q2, left panel, or Q3, right panel, derived from three experiments; n=28–47) as in H. *P<0.05; **P<0.01. Error bars indicate s.e.m.

phosphorylation of both the N-terminal and the C-terminal tyrosine residues, each mediating a distinct effect. Previously, it has been demonstrated for Q3 that the two tyrosine residues must be phosphorylatable in order for the Src action to occur, as Src action was inhibited in channels bearing single non-phosphorylatable mutations of either one of the tyrosine residues (Li et al., 2004). In this study, using the corresponding Q2 non-phosphorylatable mutants, we demonstrate that this also applies to Src action on Q2, at the levels of macroscopic currents (Fig. 3B), single-channel gating (*Po*; Fig. 3D) and at the structural level of N-terminus–C-terminus interactions (FRET; Fig. 6D,E). Furthermore, we demonstrate that it does not reflect constraints of the intrinsic channel gating mechanism, rather, it is set by Src itself, as the *Po* of the double mutant Q2-Y74D;Q2-Y347F significantly increased as mediated by the N-terminal phosphomimetic substitution even in the presence of the C-terminal non-phosphorylatable substitution

Journal of Cell Science (2015) 128, 3489-3501 doi:10.1242/jcs.173922

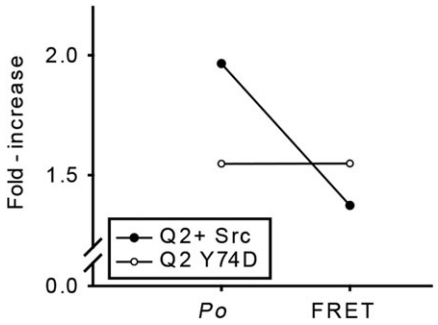

Fig. 7. Concurrent phosphorylation of both N-terminal and C-terminal tyrosine residues mediates the effect of Src on Q2. Phosphomimetic substitution of the N-terminal tyrosine (Q2-Y74D) results in similar fold increases in *Po* and FRET values, whereas co-expression of Src with WT Q2 results in a smaller fold increase in FRET, compared to that in *Po*. An analysis of variance (ANOVA) was performed, with the between variables Group (Q2 Y74D vs Q2+Src) and Method (*Po* vs FRET) on the increase ratio (fold increase) as a dependent variable. The results yielded a significant main effect of Method, F (1,31)=5.09, P<0.05, mean squared error (MSE)=0.122. Importantly, the interaction between Method and Group was significant, F (1,31)=5.12, P<0.05, MSE=0.122, indicating that for Q2-Y74D there was no difference between *Po* and FRET F<1, but for Q2+Src there was a significant increase in the ratio from FRET to *Po*, F (1,31)=8.57, P<0.01, MSE=0.122.

(Fig. 5A), and the *Po* of the double mutant Q2-Y74F;Q2-Y347D decreased to zero due to the C-terminal phosphomimetic substitution (data not shown) even in the presence of N-terminal non-phosphorylatable substitution. Ultimately, by integrating *Po* with FRET analyses, we resolve the coincidence of the two effects in the Src action (Fig. 7).

The second facet of the Src mechanism confers subunit-specific regulation. Whereas the C-terminal tyrosine residues reside in a highly conserved domain between the Q2 and Q3 (Fig. 3A) and their phosphorylation exerts similar gating downregulation in both channels (Fig. 4A–C), the N-terminal tyrosine residues reside in a less-conserved domain (Fig. 3A) and exert opposite effects on Q2 and Q3 gating, up- and down-regulation, respectively (Fig. 4D,E). Furthermore, we show that the effects mediated by N-terminal tyrosine residues are highly dependent not only on the N-terminal sequences but actually require compatibility between the whole N-terminal and C-terminal sequences (Fig. 5B), arguing that rearrangements of defined cytosolic structures comprising both N- and C-termini confer the specificity of gating regulation, either up or down.

The two-faceted Src action gives rise to an intricate mechanism. Src-induced phosphorylation of the C-terminal tyrosine residue confers inhibition of currents in both channels. However, and most importantly, the requirement for two tyrosine residues to be concurrently phosphorylated confers modification of this inhibition through phosphorylation of the N-terminal tyrosine, discriminating between the effects of Src on the two channels. In Q3, the N-terminal-tyrosine-mediated inhibition reinforces the C-terminal-tyrosine-mediated inhibition, resulting in a strong reduction of Q3 currents by Src in oocytes (Fig. 1A,B) and in CHO cells (Li et al., 2004). In Q2, the N-terminal-tyrosine-mediated excitation opposes the C-terminal-tyrosine-mediated inhibition, both concurrently resulting in a range of Src effects on Q2 currents, from a subtle current reduction in oocytes (Fig. 1A,B) and a null effect in CHO cells (Gamper et al., 2003) to a tonic increase in HEK cells (Jow and Wang, 2000).

The divergent effects of Src on Q2 are in accord with a notion that the conformational transitions induced by phosphorylation of each one of the tyrosine residues by Src might be distinct, each separately influenced by cross interaction(s) with other channel regulatory or auxiliary protein(s) for which expression level(s) depend on the cellular setup of the specific cell. Future experiments in different mammalian cell lines should resolve the influence of cytosolic proteins or the cellular environment on the Src effect on Q2. One plausible cross-interacting protein could be CaM given that the C-terminal tyrosine residues are located in the domain suggested to be a site for a true CaM-mediated channel structure (Wen and Levitan, 2002; Yus-Najera et al., 2002; Gamper and Shapiro, 2003). Thus, Src-induced C-terminal tyrosine phosphorylation, which is associated in our study with impaired structure and loss of channel function, could be very well affected by cross interaction with CaM.

Mechanism of action of the N-terminal and C-terminal tyrosine residues

Examination of the gating regulations mediated by the N-terminal tyrosine residues of both Q2 and Q3 channels reveals a mode of regulation, with positive correlation between effects on channel gating (*Po*) and N-terminus–C-terminus interaction (FRET) (compare Figs 2 and 4E with Fig. 6). Thus, increased or decreased FRET signals are interpreted as increased or decreased N-terminus–C-terminus proximity. We believe (Fig. 8A), as argued previously (Etzioni et al., 2011), that changes in FRET efficiency likely report proximity rather than orientation change of the fluorescent domains, given that the FRET dependence on orientation is less of a problem when fluorescent proteins are fused to the distal ends of channel termini and hence are relatively mobile (Zheng and Zagotta, 2004). Fig. 8B depicts our view of this mode of regulation mediated by the N-terminal tyrosine residues, with closer proximity between the cytosolic terminal in Q2 or their drawing apart in Q3 underlying gating up- or down-regulations, respectively. Notably, this regulation mode is newly discovered and distinct from that utilized by CaM and Syx because it has an inverse relationship between changes in gating and N-terminus–C-terminus proximity; namely, gating down-regulation is accompanied by increased N-terminus–C-terminus proximity. The different N-terminus–C-terminus regulations might be explained in the framework of a tetrameric channel structure composed of four subunits, as different channel modulators might mediate different N-terminus–C-terminus rearrangements between and/or within channel subunits. Fig. 8C depicts our view of the regulation mediated by the C-terminal tyrosine residues with the separation between the cytosolic termini that underlying non-functional channels.

Physiological relevance of the Src-mediated regulation of M-channels

Src is expressed by virtually all cells including diverse neuronal cell types, where it is localized in dendrites, axons and nerve terminals (Sugrue et al., 1990). The very high expression levels of Src found in nerve terminals of neurons suggests that it has a role in synaptic transmission and plasticity (Purcell and Carew, 2003; Kalia et al., 2004; Ingley, 2008); however, its role and the signaling pathways that regulate its activity at the presynaptic level are poorly understood. High levels of Src are associated with synaptic vesicles and the presynaptic structures (Pang et al., 1988; Barnekow et al., 1990; Stenius et al., 1995; Onofri et al., 1997, 2007; Janz and Sudhof, 1998). High-frequency synaptic stimulation, epileptiform activity and spatial learning trials activate Src kinases and promote their association with presynaptic proteins, including synapsin I (Lauri et al., 2000;

Journal of Cell Science (2015) 128, 3489-3501 doi:10.1242/jcs.173922

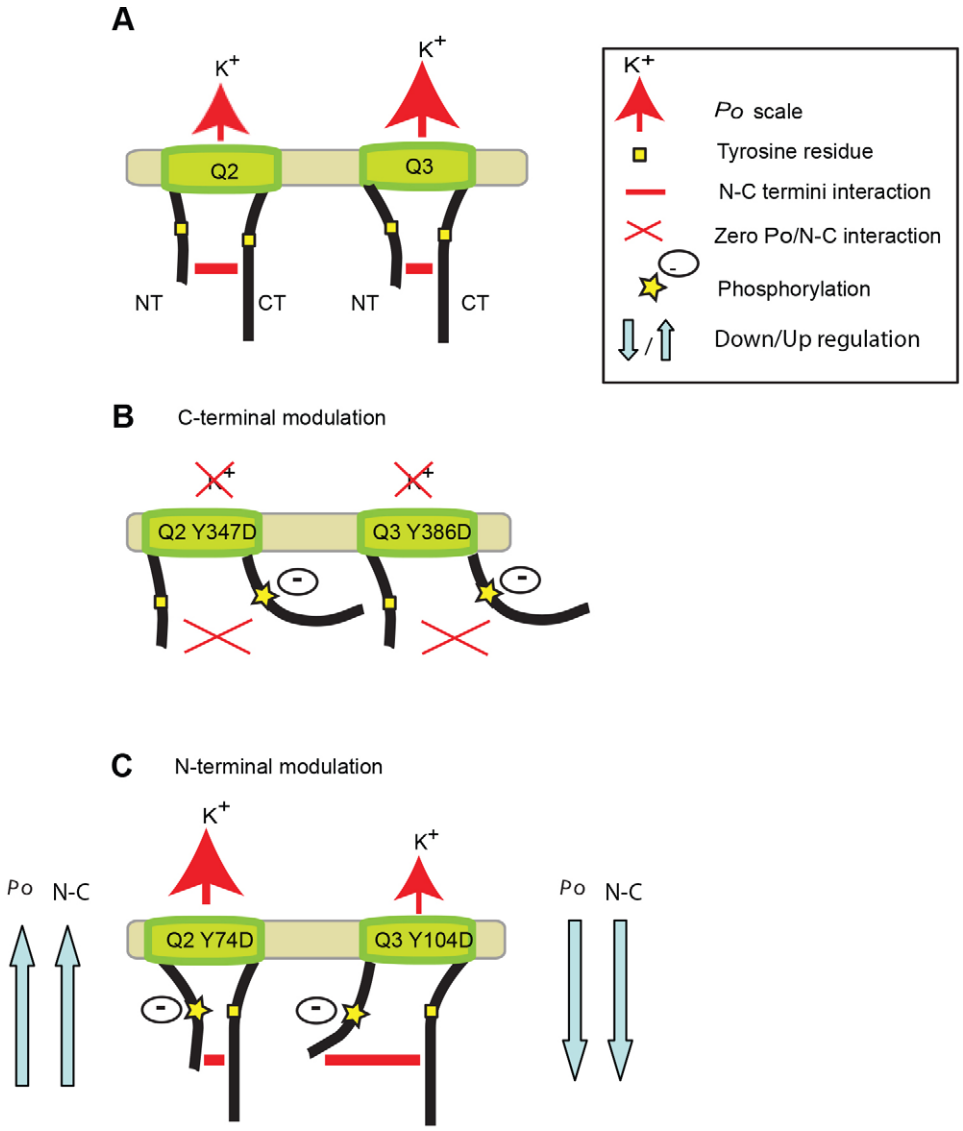

Fig. 8. Model depicting the constitutive N-terminus–C-terminus interactions and those corresponding to the Src-mediated bifunctional regulation of Q2 and Q3 through their N-terminal and C-terminal tyrosine residues. (A) Q2 and Q3 have constitutive N-terminus–C-terminus (N–C) interactions, which can be inter or intra subunit (red horizontal bars; Etzioni et al., 2011). C-terminal and N-terminal tyrosine residues are depicted by yellow squares. (B) Manipulations (phosphomimetic substitutions and possibly phosphorylations by Src; depicted by a yellow star and a negative charge) of the C-terminal tyrosine residues of Q2 and Q3 involve no N-terminus–C-terminus interactions (depicted by red X instead of red horizontal bar), accompanied by loss of channel functionality (depicted by red X over the vertical red arrows of K^+ fluxes). (C) Manipulations of the N-terminal tyrosine involve an increase in N-terminus–C-terminus proximity, accompanied by increased *Po* (depicted by larger vertical red arrow of K^+ flux) in Q2, but involve reduction in N-terminus–C-terminus proximity (larger N-terminus–C-terminus distance), accompanied by decreased *Po* (depicted by smaller vertical red arrow of K^+ flux) in Q3. Light blue arrows demonstrate upregulation of both N-terminus–C-terminus interaction and *Po* in Q2.

Sanna et al., 2000; Zhao et al., 2000). Studies using specific Src inhibitors have indicated that Src family kinases directly modulate neurotransmitter release by interfering with activity-dependent Ca^{2+} entry, actin dynamics and exocytosis (Ohnishi et al., 2001; Baldwin et al., 2006; Cheng et al., 2007, but see Wang, 2003; Shyu et al., 2005). One of the mechanisms suggested for Src regulation of neurotransmitter release is by modifying, through phosphorylation, the activity of proteins, such as the synapsins, involved in the regulation of exocytosis and synaptic vesicles trafficking (Messa et al., 2010; Bykhovskaia, 2011).

Importantly, although dynamic regulation of presynaptic voltage-gated K^+ channels, resulting in the modulation of the presynaptic voltage waveform that regulates presynaptic Ca^{2+} inflow, is an established mechanism for regulation of neurotransmitter release (e.g. Geiger and Jonas, 2000), such a mechanism has not yet been documented for Src action and is suggested here. Namely, we suggest that Src regulates neurotransmitter release through regulation of presynaptic homomeric Q2 channels (suggested to play a major role in the regulation of neurotransmitter release; see Introduction). The concurrent bidirectional regulation of Q2 by Src, mediated through two separate sites, renders it prone to modifications by cellular factors that might specifically interact with either one of the sites. A plausible candidate is CaM, which interacts with the C-terminal tyrosine site and for which levels of expression might vary among neurons and under pathophysiological conditions (Palfi et al., 2001, 2002; Kortvely and Gulya, 2004). Such modifiable Src regulation of Q2 would be nicely designed to fine-tune transmitter release.

MATERIALS AND METHODS

Constructs and antibodies

Human Q2 (Y15065) cDNAs was kindly provided by Thomas Jentsch (Zentrum für Molekulare Neuropathobiologie, Hamburg, Germany). Human $Q3_{A315T}$, $Q2_{(223)}$ and $Q2_{(322)}$ were kindly provided by Alvaro Villarroel (Unidad de Biofísica, Consejo Superior de Investigaciones Científicas–Universidad del País Vasco (UPV)/Euskal Herriko Unibersitatea, UPV, Leioa, Spain). Y527F Src was kindly provided by Sara A. Courtneidge (Sugen Inc.). All mutations and chimeras were constructed by using direct cloning of PCR (Weiner, 1993). To find homologous regions between channels, alignment was performed using CLUSTAL W (1.83) multiple sequence alignment. Tyr-74 and Tyr-347, human Q2 were found to be homologous to those in Tyr-104 and Tyr-386 human Q3 (the latter are homologous to those identified in rat Q3; Li et al., 2004). Double-fluorophore-labeled Q2 or Q3 were constructed by subcloning of native channels into pGEMHJ containing enhanced CFP

(eCFP) and enhanced YFP (eYFP) at N-terminal and C-terminal positions, respectively, through Ser-Arg linkers (encoded by XbaI restriction sites). eYFP had the Q69M mutation reducing its environmental sensitivity (Griesbeck et al., 2001). eCFP and eYFP had a A206K mutation, reducing their affinity to each other (Shaner et al., 2005). All constructs were verified by DNA sequencing. Antibodies used included anti-KCNQ2, anti-KCNQ3 (Alomone Labs) and anti-phosphotyrosine (Millipore) antibodies.

Electrophysiology

Female *Xenopus laevis* oocytes were prepared (Dascal, 1993) and proteins were expressed as previously described (Levin et al., 1995). All animal experiments were performed according to approved guidelines. The following mRNA concentrations were injected (in ng/oocyte): 7.5 Q2, 0.75 Q3, 5 Src. Two-electrode voltage-clamp analysis of macro currents was performed as previously described (Levin et al., 1995; Regev et al., 2009). Current–voltage relationships were obtained by depolarizing steps (of 1.5 s) from a holding potential of −80 to +60 mV in 10 mV increments (with 5 s intervals between episodes). Net current is obtained by subtracting the scaled leak current elicited by a voltage step from −90 to −100 mV. Oocytes with a leak current of >4 nA/1 mV are discarded. The extent of amplitude reduction was calculated as the fraction decreased. Namely, in each test group of oocytes, the mean value of current amplitude for each group was divided by the mean value of the corresponding control group (expressing channel only). The data are presented as mean±s.e.m.

Single-channel patch clamp

Cell-attached patch clamp recordings of single-channel currents were performed as previously described (Singer-Lahat et al., 1999; Michaelevski et al., 2007; Etzioni et al., 2011). The vitelline membrane of oocytes was removed and the latter were placed in a bath solution containing the following: 146 mM KCl, 2 mM NaCl, 1 mM $CaCl_2$, 1 mM $MgCl_2$, 0.1 mM EGTA, 10 mM HEPES, pH 7.5. Patch pipettes were pulled from glass capillary tubing (Sutter Instruments) with a 2–5 MΩ tip resistance. Patch pipettes were filled with solution containing 150 mM NaCl, 2 mM KCl, 1 mM $CaCl_2$, 1 mM $MgCl_2$, 5 mM HEPES, pH 7.5. Single-channel recordings were made in response to step depolarization from −90 to 0 mV for 4 s with a 5-s interval between sweeps, and the holding potential was −90 mV. Inward currents are shown as downward deflections. Data were sampled at 20 kHz and filtered with an analog Bessel filter at 5 kHz. Amplification was performed with an Axopatch 200B amplifier; and the acquired analog signal was digitized with a DigiData 1200B converter, recorded with Clampex 8.1. Analysis of the data was performed in Clampfit 10.2 (pClamp; Molecular Device) as described previously (Etzioni et al., 2011). Event detection was performed using an algorithm built-in pClamp10.2 software and the events were accepted after checking visually.

FRET analysis and confocal microscopy

FRET experiments were performed as previously described (Lvov et al., 2009). Oocytes were injected with the following mRNA concentrations (in ng/oocyte): 45 double-labeled Q2, Q3, or mutant channels, 5 Src. Fluorescence emissions from eCFP- and/or eYFP-tagged proteins were collected from the animal hemisphere of the oocyte with a confocal microscope (Ziess LSM 510 Meta), using a 20×0.75 NA objective and laser excitation of 405 and 514 nm, respectively. The level of laser intensity and the photomultiplier tube gain were kept the same for all experiments after initial calibration and titration of proteins. We used a spectrum-based method to remove contaminations caused by donor emission and direct excitation of the acceptor. The FRET assay was performed as previously described (Zheng and Zagotta, 2004). The apparent FRET efficiency from individual cells was calculated as described (Takanishi et al., 2006; Gao et al., 2007).

Peripheral channels imaging with LSM 510 was performed as previously described (Regev et al., 2009). The thickness of the optical slide was 8 µm.

Immunoprecipitation and immunoblotting

Oocytes were subjected to immunoprecipitation or immunoblotting analyses, as previously described (Levin et al., 1995; Regev et al., 2009).

Presentation and analysis of the experimental results

Statistical estimations and graphical presentation of the data were performed in SigmaStat and SigmaPlot software (Systat Software). Comparisons between two groups were tested for statistical significance ($P<0.05$ or smaller) using two-tailed unpaired or paired Student's *t*-tests according to the statistical problem requirement. Statistical evaluation of comparison of several groups was performed using one-way ANOVA followed by Bonferroni's test. Interaction between groups was evaluated using two-way ANOVA, statistical estimations of this data were performed in STATISTICA (StatSoft). The data are presented as mean±s.e.m.; *n* denotes total number of oocytes per group; *N* denotes number of experiments in different batches of oocytes.

Acknowledgements

We thank Dr Roy Luria, The School of Psychological Sciences and the Sagol School of Neuroscience, Tel-Aviv University, for kindly assisting with statistical analysis. This work was performed in partial fulfillment of the requirements for a Ph.D. degree by Sivan Siloni at the Sackler Faculty of Medicine, Tel Aviv University, Israel.

Competing interests

The authors declare no competing or financial interests.

Author contributions

S.S., D.S.-L. and I.L. conceived the project; S.S., D.S.-L. and D.C. designed the experiments; S.S, D.S.-L., M.E. and D.C. performed the experiments; S.S., D.S.-L., M.E., D.C. and V.T. analyzed data; S.S., D.S.-L. and I.L. wrote the article.

Funding

This research received no specific grant from any funding agency in the public, commercial or not-for-profit sectors.

Supplementary material

Supplementary material available online at
http://jcs.biologists.org/lookup/suppl/doi:10.1242/jcs.173922/-/DC1

References

Baldwin, M. L., Cammarota, M., Sim, A. T. R. and Rostas, J. A. P. (2006). Src family tyrosine kinases differentially modulate exocytosis from rat brain nerve terminals. *Neurochem. Int.* **49**, 80-86.

Barnekow, A., Jahn, R. and Schartl, M. (1990). Synaptophysin: a substrate for the protein tyrosine kinase pp60c-src in intact synaptic vesicles. *Oncogene* **5**, 1019-1024.

Biervert, C., Schroeder, B. C., Kubisch, C., Berkovic, S. F., Propping, P., Jentsch, T. J. and Steinlein, O. K. (1998). A potassium channel mutation in neonatal human epilepsy. *Science* **279**, 403-406.

Brown, D. A. and Adams, P. R. (1980). Muscarinic suppression of a novel voltage-sensitive K+ current in a vertebrate neurone. *Nature* **283**, 673-676.

Bykhovskaia, M. (2011). Synapsin regulation of vesicle organization and functional pools. *Semin. Cell Dev. Biol.* **22**, 387-392.

Cheng, H., Straub, S. G. and Sharp, G. W. G. (2007). Inhibitory role of Src family tyrosine kinases on Ca2+-dependent insulin release. *Am. J. Physiol. Endocrinol. Metab.* **292**, E845-E852.

Chung, H. J., Jan, Y. N. and Jan, L. Y. (2006). Polarized axonal surface expression of neuronal KCNQ channels is mediated by multiple signals in the KCNQ2 and KCNQ3 C-terminal domains. *Proc. Natl. Acad. Sci. USA* **103**, 8870-8875.

Cooper, E. C. and Jan, L. Y. (2003). M-channels: neurological diseases, neuromodulation, and drug development. *Arch. Neurol.* **60**, 496-500.

Dascal, N. (1993). Expression of exogenous ion channels and neurotransmitter receptors in RNA-injected Xenopus oocytes. *Methods Mol. Biol.* **13**, 205-225.

Devaux, J. J., Kleopa, K. A., Cooper, E. C. and Scherer, S. S. (2004). KCNQ2 is a nodal K+ channel. *J. Neurosci.* **24**, 1236-1244.

Dolly, J. O. and Parcej, D. N. (1996). Molecular properties of voltage-gated K+ channels. *J. Bioenerg. Biomembr.* **28**, 231-253.

Ebner-Bennatan, S., Patrich, E., Peretz, A., Kornilov, P., Tiran, Z., Elson, A. and Attali, B. (2012). Multifaceted modulation of K+ channels by protein-tyrosine phosphatase epsilon tunes neuronal excitability. *J. Biol. Chem.* **287**, 27614-27628.

Etxeberria, A., Santana-Castro, I., Regalado, M. P., Aivar, P. and Villarroel, A. (2004). Three mechanisms underlie KCNQ2/3 heteromeric potassium M-channel potentiation. *J. Neurosci.* **24**, 9146-9152.

Etzioni, A., Siloni, S., Chikvashvilli, D., Strulovich, R., Sachyani, D., Regev, N., Greitzer-Antes, D., Hirsch, J. A. and Lotan, I. (2011). Regulation of neuronal M-channel gating in an isoform-specific manner: functional interplay between calmodulin and syntaxin 1A. *J. Neurosci.* **31**, 14158-14171.

Gamper, N. and Shapiro, M. S. (2003). Calmodulin mediates Ca2+-dependent modulation of M-type K+ channels. *J. Gen. Physiol.* **122**, 17-31.

Gamper, N., Stockand, J. D. and Shapiro, M. S. (2003). Subunit-specific modulation of KCNQ potassium channels by Src tyrosine kinase. *J. Neurosci.* **23**, 84-95.
Gao, Y., Liu, S.-S., Qiu, S., Cheng, W., Zheng, J. and Luo, J.-H. (2007). Fluorescence resonance energy transfer analysis of subunit assembly of the ASIC channel. *Biochem. Biophys. Res. Commun.* **359**, 143-150.
Geiger, J. R. P. and Jonas, P. (2000). Dynamic control of presynaptic Ca(2+) inflow by fast-inactivating K(+) channels in hippocampal mossy fiber boutons. *Neuron* **28**, 927-939.
Griesbeck, O., Baird, G. S., Campbell, R. E., Zacharias, D. A. and Tsien, R. Y. (2001). Reducing the environmental sensitivity of yellow fluorescent protein: mechanism and applications. *J. Biol. Chem.* **276**, 29188-29194.
Hille, B. (1992). *Ion Channels of Excitable Membranes*. Sunderland, MA: Sinauer Associates.
Ingley, E. (2008). Src family kinases: regulation of their activities, levels and identification of new pathways. *Biochim. Biophys. Acta* **1784**, 56-65.
Ivanina, T., Perets, T., Thornhill, W. B., Levin, G., Dascal, N. and Lotan, I. (1994). Phosphorylation by protein kinase A of RCK1 K+ channels expressed in Xenopus oocytes. *Biochemistry* **33**, 8786-8792.
Janz, R. and Sudhof, T. C. (1998). Cellugyrin, a novel ubiquitous form of synaptogyrin that is phosphorylated by pp60c-src. *J. Biol. Chem.* **273**, 2851-2857.
Jentsch, T. J. (2000). Neuronal KCNQ potassium channels: physiology and role in disease. *Nat. Rev.* **1**, 21-30.
Jow, F. and Wang, K.-W. (2000). Cloning and functional expression of rKCNQ2 K(+) channel from rat brain. *Brain Res. Mol. Brain Res.* **80**, 269-278.
Kalia, L. V., Gingrich, J. R. and Salter, M. W. (2004). Src in synaptic transmission and plasticity. *Oncogene* **23**, 8007-8016.
Klinger, F., Gould, G., Boehm, S. and Shapiro, M. S. (2011). Distribution of M-channel subunits KCNQ2 and KCNQ3 in rat hippocampus. *Neuroimage* **58**, 761-769.
Kortvely, E. and Gulya, K. (2004). Calmodulin, and various ways to regulate its activity. *Life Sci.* **74**, 1065-1070.
Lauri, S. E., Taira, T. and Rauvala, H. (2000). High-frequency synaptic stimulation induces association of fyn and c-src to distinct phosphorylated components. *Neuroreport* **11**, 997-1000.
Levin, G., Keren, T., Peretz, T., Chikvashvili, D., Thornhill, W. B. and Lotan, I. (1995). Regulation of RCK1 currents with a cAMP analog via enhanced protein synthesis and direct channel phosphorylation. *J. Biol. Chem.* **270**, 14611-14618.
Li, Y., Langlais, P., Gamper, N., Liu, F. and Shapiro, M. S. (2004). Dual phosphorylations underlie modulation of unitary KCNQ K(+) channels by Src tyrosine kinase. *J. Biol. Chem.* **279**, 45399-45407.
Lippiat, J. D., Albinson, S. L. and Ashcroft, F. M. (2002). Interaction of the cytosolic domains of the Kir6.2 subunit of the K(ATP) channel is modulated by sulfonylureas. *Diabetes* **51** Suppl. 3, S377-S380.
Lvov, A., Greitzer, D., Berlin, S., Chikvashvili, D., Tsuk, S., Lotan, I. and Michaelevski, I. (2009). Rearrangements in the relative orientation of cytoplasmic domains induced by a membrane-anchored protein mediate modulations in Kv channel gating. *J. Biol. Chem.* **284**, 28276-28291.
Marrion, N. V. (1997). Control of M-current. *Annu. Rev. Physiol.* **59**, 483-504.
Martire, M., Castaldo, P., D'Amico, M., Preziosi, P., Annunziato, L. and Taglialatela, M. (2004). M channels containing KCNQ2 subunits modulate norepinephrine, aspartate, and GABA release from hippocampal nerve terminals. *J. Neurosci.* **24**, 592-597.
Messa, M., Congia, S., Defranchi, E., Valtorta, F., Fassio, A., Onofri, F. and Benfenati, F. (2010). Tyrosine phosphorylation of synapsin I by Src regulates synaptic-vesicle trafficking. *J. Cell Sci.* **123**, 2256-2265.
Michaelevski, I., Korngreen, A. and Lotan, I. (2007). Interaction of syntaxin with a single Kv1.1 channel: a possible mechanism for modulating neuronal excitability. *Pflugers Arch.* **454**, 477-494.
Millar, I. D., Bruce, J. and Brown, P. D. (2007). Ion channel diversity, channel expression and function in the choroid plexuses. *Cerebrospinal Fluid Res.* **4**, 8.
Miller, C. (2000). An overview of the potassium channel family. *Genome Biol.* **1**, reviews0004-reviews0004.5.
Ohnishi, H., Yamamori, S., Ono, K., Aoyagi, K., Kondo, S. and Takahashi, M. (2001). A src family tyrosine kinase inhibits neurotransmitter release from neuronal cells. *Proc. Natl. Acad. Sci. USA* **98**, 10930-10935.
Onofri, F., Giovedi, S., Vaccaro, P., Czernik, A. J., Valtorta, F., De Camilli, P., Greengard, P. and Benfenati, F. (1997). Synapsin I interacts with c-Src and stimulates its tyrosine kinase activity. *Proc. Natl. Acad. Sci. USA* **94**, 12168-12173.
Onofri, F., Messa, M., Matafora, V., Bonanno, G., Corradi, A., Bachi, A., Valtorta, F. and Benfenati, F. (2007). Synapsin phosphorylation by SRC tyrosine kinase enhances SRC activity in synaptic vesicles. *J. Biol. Chem.* **282**, 15754-15767.
Palfi, A., Simonka, J. A., Pataricza, M., Tekulics, P., Lepran, I., Papp, G. and Gulya, K. (2001). Postischemic calmodulin gene expression in the rat hippocampus. *Life Sci.* **68**, 2373-2381.
Palfi, A., Kortvely, E., Fekete, E., Kovacs, B., Varszegi, S. and Gulya, K. (2002). Differential calmodulin gene expression in the rodent brain. *Life Sci.* **70**, 2829-2855.
Pang, D. T., Wang, J. K., Valtorta, F., Benfenati, F. and Greengard, P. (1988). Protein tyrosine phosphorylation in synaptic vesicles. *Proc. Natl. Acad. Sci. USA* **85**, 762-766.
Peretz, A., Sheinin, A., Yue, C., Degani-Katzav, N., Gibor, G., Nachman, R., Gopin, A., Tam, E., Shabat, D., Yaari, Y. et al. (2007). Pre- and postsynaptic activation of M-channels by a novel opener dampens neuronal firing and transmitter release. *J. Neurophysiol.* **97**, 283-295.
Purcell, A. L. and Carew, T. J. (2003). Tyrosine kinases, synaptic plasticity and memory: insights from vertebrates and invertebrates. *Trends Neurosci.* **26**, 625-630.
Regev, N., Degani-Katzav, N., Korngreen, A., Etzioni, A., Siloni, S., Alaimo, A., Chikvashvili, D., Villarroel, A., Attali, B. and Lotan, I. (2009). Selective interaction of syntaxin 1A with KCNQ2: possible implications for specific modulation of presynaptic activity. *PLoS ONE* **4**, e6586.
Robbins, J. (2001). KCNQ potassium channels: physiology, pathophysiology, and pharmacology. *Pharmacol. Ther.* **90**, 1-19.
Rubinstein, M., Peleg, S., Berlin, S., Brass, D., Keren-Raifman, T., Dessauer, C. W., Ivanina, T. and Dascal, N. (2009). Divergent regulation of GIRK1 and GIRK2 subunits of the neuronal G protein gated K+ channel by GalphaiGDP and Gbetagamma. *J. Physiol.* **587**, 3473-3491.
Sanna, P. P., Berton, F., Cammalleri, M., Tallent, M. K., Siggins, G. R., Bloom, F. E. and Francesconi, W. (2000). A role for Src kinase in spontaneous epileptiform activity in the CA3 region of the hippocampus. *Proc. Natl. Acad. Sci. USA* **97**, 8653-8657.
Shaner, N. C., Steinbach, P. A. and Tsien, R. Y. (2005). A guide to choosing fluorescent proteins. *Nat. Methods* **2**, 905-909.
Shyu, K.-G., Jow, G.-M., Lee, Y.-J. and Wang, S.-J. (2005). PP2 inhibits glutamate release from nerve endings by affecting vesicle mobilization. *Neuroreport* **16**, 1969-1972.
Singer-Lahat, D., Dascal, N. and Lotan, I. (1999). Modal behavior of the Kv1.1 channel conferred by the Kvbeta1.1 subunit and its regulation by dephosphorylation of Kv1.1. *Pflugers Arch.* **439**, 18-26.
Singh, N. A., Charlier, C., Stauffer, D., DuPont, B. R., Leach, R. J., Melis, R., Ronen, G. M., Bjerre, I., Quattlebaum, T., Murphy, J. V. et al. (1998). A novel potassium channel gene, KCNQ2, is mutated in an inherited epilepsy of newborns. *Nat. Genet.* **18**, 25-29.
Stenius, K., Janz, R., Sudhof, T. C. and Jahn, R. (1995). Structure of synaptogyrin (p29) defines novel synaptic vesicle protein. *J. Cell Biol.* **131**, 1801-1809.
Sugrue, M. M., Brugge, J. S., Marshak, D. R., Greengard, P. and Gustafson, E. L. (1990). Immunocytochemical localization of the neuron-specific form of the c-src gene product, pp60c-src(+), in rat brain. *J. Neurosci.* **10**, 2513-2527.
Takanishi, C. L., Bykova, E. A., Cheng, W. and Zheng, J. (2006). GFP-based FRET analysis in live cells. *Brain Res.* **1091**, 132-139.
Tsuboi, T., Lippiat, J. D., Ashcroft, F. M. and Rutter, G. A. (2004). ATP-dependent interaction of the cytosolic domains of the inwardly rectifying K+ channel Kir6.2 revealed by fluorescence resonance energy transfer. *Proc. Natl. Acad. Sci. USA* **101**, 76-81.
Wang, S.-J. (2003). A role for Src kinase in the regulation of glutamate release from rat cerebrocortical nerve terminals. *Neuroreport* **14**, 1519-1522.
Wang, H.-S., Pan, Z., Shi, W., Brown, B. S., Wymore, R. S., Cohen, I. S., Dixon, J. E. and McKinnon, D. (1998). KCNQ2 and KCNQ3 potassium channel subunits: molecular correlates of the M-channel. *Science* **282**, 1890-1893.
Weckhuysen, S., Mandelstam, S., Suls, A., Audenaert, D., Deconinck, T., Claes, L. R. F., Deprez, L., Smets, K., Hristova, D., Yordanova, I. et al. (2012). KCNQ2 encephalopathy: emerging phenotype of a neonatal epileptic encephalopathy. *Ann. Neurol.* **71**, 15-25.
Weiner, M. P. (1993). Directional cloning of blunt-ended PCR products. *BioTechniques* **15**, 502-505.
Wen, H. and Levitan, I. B. (2002). Calmodulin is an auxiliary subunit of KCNQ2/3 potassium channels. *J. Neurosci.* **22**, 7991-8001.
Yus-Najera, E., Santana-Castro, I. and Villarroel, A. (2002). The identification and characterization of a noncontinuous calmodulin-binding site in noninactivating voltage-dependent KCNQ potassium channels. *J. Biol. Chem.* **277**, 28545-28553.
Zhao, W., Cavallaro, S., Gusev, P. and Alkon, D. L. (2000). Nonreceptor tyrosine protein kinase pp60c-src in spatial learning: synapse-specific changes in its gene expression, tyrosine phosphorylation, and protein-protein interactions. *Proc. Natl. Acad. Sci. USA* **97**, 8098-8103.
Zheng, J. and Zagotta, W. N. (2004). Stoichiometry and assembly of olfactory cyclic nucleotide-gated channels. *Neuron* **42**, 411-421.